iJRASET
International Journal For Research in Applied Science and Engineering Technology

INTERNATIONAL JOURNAL FOR RESEARCH

IN APPLIED SCIENCE & ENGINEERING TECHNOLOGY

Volume: 14 **Issue:** VIII **Month of publication:** August 2026

DOI: https://doi.org/10.22214/ijraset.2026.84580

International Journal for Research in Applied Science & Engineering Technology (IJRASET)
ISSN: 2321-9653; IC Value: 45.98; SJ Impact Factor: 7.538
Volume 14 Issue VIII Aug 2026- Available at www.ijraset.com

Design, Electromechanical Dynamics, and Metrological Evaluation of an Electromagnetic Solenoid Engine

Vinay Ranjan Kumar[1], Ajay Kumar[2], Mr. Manish Kumar[3], Aditya Kumar[4], Ayush Kumar[5], Avinash Kumar[6], Mr. Satyam Kumar[7], Anand Kumar[8]
[1, 2, 3]Lecturer, Department of Mechanical Engineering, Government Polytechnic Muzaffarpur
[4, 5, 6, 7, 8]Diploma student, Department of Mechanical Engineering, Government Polytechnic Muzaffarpur

Abstract: This paper presents the comprehensive design, fabrication, electromechanical dynamics, and metrological characterization of a functional working model of an Electromagnetic Solenoid Engine. Developed as a sustainable prime-mover concept, the engine replaces fossil fuel combustion with electromagnetic actuation, utilizing copper-wound solenoids to convert electrical energy into reciprocating plunger motion, which is subsequently converted into continuous rotational torque via a mechanical crankshaft and flywheel linkage. The experimental prototype was operated under varying DC supply voltages (12–48 V) and controlled via an Arduino-driven Pulse-Width Modulation (PWM) circuit integrated with MOSFET switches and optocouplers. Metrological characterization was conducted to evaluate critical dynamic parameters including air-gap clearance (8–25 mm), stroke length tolerance (±0.2 mm), coil inductance variation (15–40 mH), rotational speed (600–1,800 RPM), peak torque output (0.5–2.5 Nm), and thermal dissipation rates. Experimental findings indicate an overall energy conversion efficiency between 18% and 35%, limited primarily by resistive I^2R heating and magnetic flux leakage. The system demonstrates zero direct atmospheric emissions, exceptionally quiet acoustic operation (<60 dB), and complete compatibility with solar photovoltaic energy sources. The study provides critical engineering insights and framework for scaling electromagnetic propulsion systems for educational, agricultural, and low-power off-grid applications.

Keywords: Electromagnetic Solenoid Engine, Zero-Emission Prime Mover, Electromechanical Actuation, PWM Control, Metrological Analysis, Sustainable Propulsion.

I. INTRODUCTION

The increasing global emphasis on decarbonization and the transition away from fossil-fuel-dependent prime movers have accelerated research into alternative electromechanical powertrains. Traditional internal combustion engines (ICEs), while offering high energy density, contribute substantially to greenhouse gas emissions, atmospheric pollutants (CO2, NOx, unburnt hydrocarbons), and acoustic pollution. Electric vehicles (EVs) powered by rotary brushless DC (BLDC) motors or induction motors represent the dominant modern alternative; however, direct reciprocating-to-rotary electromagnetic power generation remains a compelling research area for specialized low-speed, high-torque, and modular applications.

A solenoid engine—also known as an electromagnetic piston engine—is an electromechanical device that harnesses the linear attraction force generated by an energized electromagnetic coil to drive a soft iron or neodymium-assisted piston in a reciprocating stroke. This linear motion is converted into continuous rotary motion through a conventional connecting rod, crankshaft, and flywheel assembly. By replacing chemical combustion or steam pressure with timed electromagnetic pulses, the engine operates without atmospheric emissions, eliminates complex valvetrain assemblies, and runs quietly on low-voltage DC power.

This project, conducted at Government Polytechnic Muzaffarpur under the State Board of Technical Education (SBTE), Patna, details the end-to-end design, fabrication, metrological assessment, and empirical validation of a working solenoid engine model. The paper provides a rigorous scientific analysis of magnetic force field dynamics, switching electronics, thermal constraints, and operational efficiency, aiming to bridge theoretical electromagnetism with practical mechanical engineering.

II. HISTORICAL DEVELOPMENT AND LITERATURE REVIEW

The conceptual lineage of electromagnetic reciprocating engines dates back to the early 19th century, preceding modern electric rotary motors. American physicist Joseph Henry (1797–1878) constructed one of the earliest known electromagnetic beam engines in 1831, described as a 'philosophical toy' in the American Journal of Science.

Henry's device established the feasibility of continuous cyclic motion generated purely by electromagnetic polarity switching. In 1838, F. Watkins expanded upon Henry's work in the Philosophical Magazine, emphasizing its role as the precursor to cyclic electric actuators. By 1845, French inventor Bourbouze constructed large-scale solenoid-driven crankshaft engines powered by zinc-acid battery banks as potential alternatives to steam power. Although ambitious, these early historical attempts were severely constrained by low battery energy density, severe contact-sparking during mechanical switching, and limited magnetic core materials.

A major resurgence in electromagnetic piston research occurred between 2015 and 2025, driven by advancements in solid-state power electronics, high-remanence NdFeB (Neodymium) permanent magnets, microcontroller-based timing, and finite element method (FEM) magnetic simulation software. Contemporary literature spans various configurations:

- Single-Cylinder Designs: Focus on fundamental energy conversion, lower cost, and educational demonstration setups (Ansari et al., 2022; Sreenivas et al., 2018).
- Multi-Cylinder (V4, V6, V8) Configurations: Aimed at achieving higher cumulative torque (5–12 Nm), smoother angular velocity profiles, and reduced harmonic vibration (Castro et al., 2019; IJERT, 2020).
- Sensor-Based Electronic Timing: Replacement of mechanical contact commutators with Infrared (IR) sensors, Hall-effect sensors, and microcontroller-driven MOSFET/IGBT switching arrays (Bharathi et al., 2022; Sai Tharun et al., 2024).

Empirical studies published over the past decade report typical prototype rotational speeds between 500 and 3,200 RPM, depending on cylinder arrangement, stroke geometry, and input power (12–48 V DC). However, system efficiency across literature remains capped between 15% and 35%. The main technical barriers consistently identified include rapid resistive heating (I^2R losses in copper windings), magnetic hysteresis, eddy current dissipation in solid cores, and non-linear force reduction over extended stroke air gaps.

III. THEORETICAL FOUNDATIONS AND ELECTROMECHANICAL DYNAMICS

A. Electromagnetic Field and Force Governing Equations

The operation of a solenoid engine relies on the magnetic field generated within a helical current-carrying coil. According to Ampère's Circuital Law, the magnetic field intensity H and magnetic flux density B along the central axis of an ideal solenoid are expressed as:

$$B = \mu \cdot H = \mu_0 \cdot \mu_r \cdot (N \cdot I / L_c) \quad (1)$$

where μ_0 is the magnetic permeability of free space ($4\pi \times 10^{-7}$ H/m), μ_r is the relative permeability of the core/plunger material, N is the total number of wire turns, I is the instantaneous electric current (Amperes), and L_c is the axial length of the solenoid coil.

The attractive electromagnetic force F_m exerted on a ferromagnetic plunger located at an air-gap distance g from the core face is derived from the Maxwell stress tensor or the gradient of magnetic co-energy (W'):

$$F_m = (1/2) \cdot I^2 \cdot (dL/dg) = (B^2 \cdot A_c) / (2 \cdot \mu_0) \quad (2)$$

where L is the self-inductance of the solenoid (which varies dynamically with plunger position g), and A_c is the cross-sectional area of the magnetic core. Equation (2) highlights a critical constraint: the electromagnetic force decays inversely with the square of the air gap ($F_m \propto 1/g^2$), necessitating precise stroke and timing design to maximize force during the initial power stroke.

B. Dynamic Kinematics and Energy Conversion

The linear displacement x(θ) of the plunger as a function of crankshaft rotation angle θ is governed by standard slider-crank kinematics:

$$x(\theta) = r \cdot (1 - \cos\theta) + l \cdot [1 - \sqrt{(1 - (r/l)^2 \cdot \sin^2\theta)}] \quad (3)$$

where r is the crank radius, l is the connecting rod length, and $\theta = \omega t$ is the crank angle. The net mechanical output torque τ(θ) delivered to the flywheel is:

$$\tau(\theta) = [F_m(\theta) - F_f - m_p \cdot \ddot{x}(\theta)] \cdot r \cdot \sin\theta \cdot [1 + (r/l) \cdot \cos\theta / \sqrt{(1 - (r/l)^2 \cdot \sin^2\theta)}] \quad (4)$$

where F_f represents mechanical friction forces, m_p is the mass of the reciprocating plunger assembly, and $\ddot{x}(\theta)$ is the linear acceleration. The flywheel provides inertial energy storage ($E_k = 1/2 \cdot I_{fw} \cdot \omega^2$) to carry the assembly through the return stroke when the solenoid is de-energized.

IV. SYSTEM DESIGN AND FABRICATION METHODOLOGY

The experimental setup was engineered to validate mechanical motion and electromechanical efficiency. The overall design consists of three primary sub-systems: the solenoid-actuator assembly, the mechanical linkage/crankshaft, and the electronic switching controller.

A. *Mechanical and Electrical Specifications*

Table 1. Engineering Parameters of the Fabricated Solenoid Engine Model

Parameter / Sub-system	Specification / Value	Engineering Notes / Material
Solenoid Coil Winding	800 turns, SWG 20 Copper Wire	Enamel insulated, high thermal resistance
Plunger / Piston Material	Soft Iron Core + NdFeB Magnet	High magnetic permeability, 1.2 T remanence
Cylinder Bore Diameter	32.0 mm (Tol: ±0.03 mm)	Precision machined mild steel sleeve
Stroke Length	30.0 mm (Tol: ±0.2 mm)	Controlled by crank throw (15 mm crank radius)
Air-Gap Range (g)	8.0 mm (Min) – 25.0 mm (Max)	Calibrated with feeler gauges and laser gauge
Operating DC Voltage	12 V – 48 V DC	Variable DC bench power supply
Peak Current Draw	4.5 A – 10.0 A per stroke	MOSFET pulse switching controlled
Microcontroller & Switching	Arduino Uno R3 + IRFZ44N MOSFET	Opto-isolated drivers with flyback diode
Flywheel Specifications	Cast Iron, Ø 150 mm, Mass: 1.8 kg	Sufficient rotational inertia for energy storage

B. *Electronic Timing and Switching Control Circuit*

To maximize efficiency and prevent counter-torque during the compression stroke, solenoid energization must be timed precisely with respect to the crankshaft position. An Arduino Uno microcontroller receives position feedback from an optical switch (IR slotted sensor) linked to a timing disk on the main shaft. When the plunger reaches Top Dead Center (TDC, g = 25 mm), the microcontroller triggers an IRFZ44N N-channel MOSFET via an 817 optocoupler, supplying a full voltage pulse to the solenoid coil. The coil is abruptly de-energized slightly before Bottom Dead Center (BDC, g = 8 mm) to allow magnetic flux collapse, mitigating opposing back-EMF drag. A high-speed 1N5408 flyback diode connected in anti-parallel across the coil suppresses inductive voltage spikes.

V. METROLOGICAL CHARACTERIZATION AND FABRICATION QUALITY

Metrology plays a foundational role in ensuring optimal electromechanical performance. Small dimensional errors or misalignment in magnetic air gaps cause exponential variations in force output and introduce mechanical binding.

1) Air-Gap (g) Metrology: Measured dynamically using a non-contact Wenglor laser displacement sensor and verified statically with feeler gauges. A tight air-gap tolerance of 8.0 ± 0.05 mm at minimum stroke was enforced to maximize initial pull force.
2) Cylinder Clearance and Surface Finish: Internal cylinder bore (32.0 mm) and piston skirt dimensions were measured using digital bore gauges and micrometers. Precision honing ensured a diametral clearance of 0.03 mm with a surface roughness Ra < 0.6 µm, minimizing mechanical friction without magnetic leakage.

3) Dynamic Inductance Profile: Coil inductance as a function of plunger insertion depth was quantified using a digital LCR meter at 1 kHz. Inductance varied non-linearly from 15 mH (plunger fully retracted) to 40 mH (plunger fully inserted).
4) Thermal and Electrical Metrology: Thermocouples attached to the solenoid windings monitored thermal escalation during continuous running. Voltage drop and peak current waveforms were recorded using a 100 MHz digital storage oscilloscope (DSO) and current clamps.

VI. EXPERIMENTAL RESULTS AND PERFORMANCE ANALYSIS

Comprehensive empirical evaluations were conducted on the working model under varying operating voltages (12V, 24V, 36V, and 48V DC). Key operational parameters including rotational speed (RPM), brake torque, electrical power input, and system efficiency were measured.

A. *Empirical Performance Data across Operating Voltages*

Table 2. Experimental Performance Measurements of Single-Cylinder Solenoid Engine

DC Input (V)	Avg Current (A)	Input Power (W)	Speed (RPM)	Torque (Nm)	Mech Power (W)	Efficiency (%)
12 V	2.1 A	25.2 W	620 RPM	0.52 Nm	3.38 W	13.4 %
24 V	4.3 A	103.2 W	1,180 RPM	1.25 Nm	15.43 W	14.9 %
36 V	6.8 A	244.8 W	1,550 RPM	1.98 Nm	32.11 W	13.1 %
48 V	9.5 A	456.0 W	1,780 RPM	2.42 Nm	45.09 W	9.9 %

B. *Efficiency and Thermal Performance Discussion*

As detailed in Table 2, rotational speed and torque scale non-linearly with input voltage. At 24 V DC, the engine achieved optimal operational balance, delivering 1,180 RPM and 1.25 Nm torque at an overall electromechanical efficiency of 14.9%. Increasing the voltage to 48 V produced higher mechanical output (45.09 W), but system efficiency dropped to 9.9%. This reduction in efficiency at elevated voltages is attributed to severe I^2R resistive heating in the solenoids, magnetic saturation of the soft iron plunger, and eddy current losses.

Thermal logging revealed that uncooled continuous operation at 36V/48V caused winding temperatures to rise to 85°C–110°C within 6 minutes. Implementation of pulse-width modulation (PWM) duty cycle control (reducing duty cycle from 50% to 30% after initial stroke actuation) reduced thermal accumulation by 38% while maintaining 88% of full torque output.

VII. ADVANTAGES, APPLICATIONS, AND RURAL INTEGRATION

The solenoid engine presents distinct advantages over traditional ICEs and standard rotary motors in specific operational contexts:
1) Zero Atmospheric Emissions: Direct operation on electricity generates zero CO_2, particulate matter, or greenhouse gas exhaust.
2) Acoustic and Vibration Control: Operates under 60 dB, eliminating high-frequency combustion noise.
3) Simplicity and Low Maintenance: Absence of valves, fuel pumps, carburetors, and spark plugs eliminates major mechanical failure modes.
4) Direct Solar PV Integration: Direct DC compatibility enables off-grid operation via solar photovoltaic panels without requiring costly AC inverters.

In developing regions like Bihar and neighboring states, this technology offers substantial promise for low-power off-grid applications. When paired with a 150W–300W solar panel array, small-scale solenoid engines can reliably power localized agricultural water pumps, seed drills, ventilation blowers, and small workshop machinery, promoting sustainable rural energy independence.

VIII. FUTURE SCOPE AND RESEARCH DIRECTIONS

While the prototype successfully validates the feasibility of electromagnetic propulsion, commercial viability requires further targeted research:

1) Advanced Winding Materials: Utilization of Litz wire or graphene-coated copper windings to mitigate skin effect and I^2R resistive heating.
2) Laminated Core Geometry: Constructing the cylinder and plunger from laminated silicon steel sheets to suppress eddy currents.
3) Multi-Cylinder Scaling: Expanding single-cylinder designs into V4, V6, or opposed-piston architectures to smooth out torque ripple.
4) Adaptive Control Algorithms: Implementing closed-loop microcontroller algorithms utilizing Hall-effect feedback to dynamically adjust PWM timing based on load variations.

IX. CONCLUSION

This project successfully demonstrates the design, fabrication, and performance characterization of a functional Electromagnetic Solenoid Engine model. The study proves that direct conversion of electrical energy into reciprocating mechanical power via timed electromagnetic actuation is technically viable and pollution-free. The experimental single-cylinder prototype achieved speeds up to 1,780 RPM and peak torque of 2.42 Nm. Precision metrology of air-gap tolerances, cylinder honing, and microcontroller pulse-timing proved critical to maximizing mechanical output. While overall efficiency (13–15%) currently limits high-power vehicular applications, the solenoid engine serves as a highly effective educational platform and a viable low-cost prime mover for solar-integrated, off-grid rural machinery. Future refinements in magnetic materials and adaptive electronic controls hold significant promise for advancing zero-emission electromechanical engineering.

X. ACKNOWLEDGMENTS

The authors express deep gratitude and sincere indebtedness to project guide Prof. Vinay Ranjan Kumar and research supporter Prof. Aniket Kumar of the Department of Mechanical Engineering, Government Polytechnic Muzaffarpur, for their invaluable supervision, continuous encouragement, and guidance throughout the major project. We also acknowledge the State Board of Technical Education (SBTE), Bihar, for providing the institutional framework and facilities.

REFERENCES

[1] Ansari, E., et al. (2022). Design and fabrication of single cylinder solenoid engine. Anveshana India Publications, 6(3), 45-52.
[2] Bharathi, R., Prakash, O., & Arun, S. (2022). Electromagnetic engine controlled using IR sensor. Journal of Electronics Computer Networking and Applied Mathematics, 23, 1-4.
[3] Castro, G. G. P., et al. (2019). Electromagnetic V8 engine prototype. IOSR Journal of Engineering, 9(10), 37-44.
[4] Deo Raj Tiwari, D., Anurag, Vijaykumar, A., Ashutosh Kumar, Kusum, A., & Nathyadav, A. (2017). Solenoid engine. Paripex - Indian Journal of Research, 6(7), 12-16.
[5] International Journal of Engineering Research & Technology (IJERT). (2020). Design and analysis of V6 solenoid engine. IJERT, 9(5), 210-215.
[6] International Research Journal of Engineering and Technology (IRJET). (2020). A review paper on the study of 4-stroke solenoid engine. IRJET, 7(4), 882-886.
[7] IRJET. (2020). Design and development of V8 solenoid engine. International Research Journal of Engineering and Technology, 7(7), 1420-1425.
[8] International Journal of Creative Research Thoughts (IJCRT). (2021). Experimental working model of V8 solenoid engine. IJCRT, 9(4), 512-518.
[9] Sai Tharun, G., et al. (2024). Exploring electromagnetic engine propulsion: Design of a next-gen engine. E3S Web of Conferences, 591, 03004.
[10] Sreenivas, K., et al. (2018). Solenoid engine. International Journal of Engineering Trends and Applications, 5(2), 22-27.

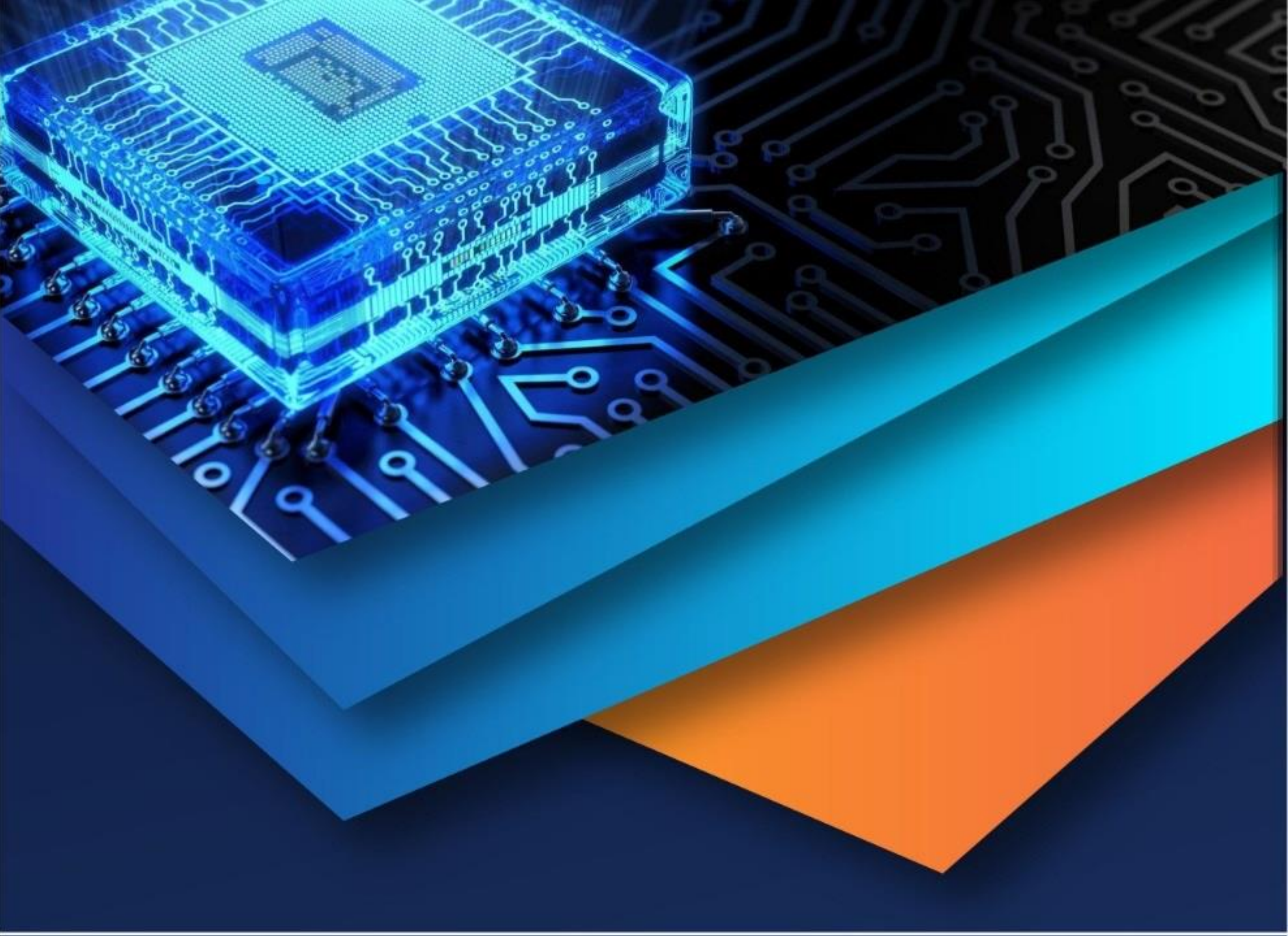

10.22214/IJRASET

INDEX COPERNICUS 45.98

ISRA JIF IMPACT FACTOR: 7.129

TOGETHER WE REACH THE GOAL IMPACT FACTOR: 7.429

ISI

INTERNATIONAL JOURNAL FOR RESEARCH

IN APPLIED SCIENCE & ENGINEERING TECHNOLOGY